ARTICLE **Communicated by Rafal Bogacz**

Sequential Effects in Two-Choice Reaction Time Tasks: Decomposition and Synthesis of Mechanisms

Juan Gao*
juangao@stanford.edu
Department of Mechanical and Aerospace Engineering and Princeton Neuroscience Institute, Princeton University, Princeton, NJ 08544, U.S.A.

KongFatt Wong-Lin
kfwong@princeton.edu
Princeton Neuroscience Institute and Program in Applied and Computational Mathematics, Princeton University, Princeton, NJ 08544, U.S.A.

Philip Holmes
pholmes@math.princeton.edu
Department of Mechanical and Aerospace Engineering, Princeton Neuroscience Institute, and Program in Applied and Computational Mathematics, Princeton University, Princeton, NJ 08544, U.S.A.

Patrick Simen
psimen@math.princeton.edu
Jonathan D. Cohen
jdc@princeton.edu
Princeton Neuroscience Institute and Department of Psychology, Princeton University, Princeton, NJ 08544, U.S.A.

Performance on serial tasks is influenced by first- and higher-order sequential effects, respectively, due to the immediately previous and earlier trials. As response-to-stimulus interval (RSI) increases, the pattern of reaction times transits from a benefit-only mode, traditionally ascribed to automatic facilitation (AF), to a cost-benefit mode, due to strategic expectancy (SE). To illuminate the sources of such effects, we develop a connectionist network of two mutually inhibiting neural decision units subject to feedback from previous trials. A study of separate biasing mechanisms shows that residual decision unit activity can lead to only first-order AF, but higher-order AF can result from strategic priming mediated by conflict monitoring, which we instantiate in two distinct versions. A further mechanism mediates expectation-related biases that grow

*Juan Gao, the corresponding author, is now at the Department of Psychology, Stanford University, Stanford, CA 94305-2130.

during RSI toward saturation levels determined by weighted repetition (or alternation) sequence lengths. Equipped with these mechanisms, the network, consistent with known neurophysiology, accounts for several sets of behavioral data over a wide range of RSIs. The results also suggest that practice speeds up all the mechanisms rather than adjusting their relative strengths.

1 Introduction

Even when subjects are instructed that stimulus sequences are randomly ordered, their reaction times (RTs) and error rates (ERs) on serial RT tasks typically depend on previous trials in a systematic manner. This sequential effect has been widely tested under different conditions and with various auditory and visual stimuli (Soetens, Boer, & Hueting, 1985; Sommer, Leuthold, & Soetens, 1999; Cho et al., 2002). Most of the literature on such effects concerns two-alternative forced-choice (2AFC) tasks, and stimulus sequences are represented using repetition (*R*) and alternation (*A*) to indicate whether a given trial is a repetition or alternation of the previous one. We follow this convention, denoting the two response choices by "1" and "2."

Sequential effects can be categorized as first order (caused by the immediately previous trial) or higher order (caused by trials earlier in the sequence). In 2AFC tasks, sequential effects are also found to vary systematically with response-to-stimulus interval (RSI), the delay between response and stimulus onset in the following trial (Kirby, 1972; Soetens et al., 1985). For short RSIs, one-sided patterns are observed, in which the response in the current trial is faster following certain sequences relative to others. For first-order effects, repetitions are faster than alternations, while for higher-order effects, responses after repetitions are faster regardless of whether the current trial is a repetition or an alternation. For example, after the sequence 1-1-1 (or 2-2-2), the response to another 1 or 2 is faster than that after 1-2-1. This one-sided effect, which reduces mean RTs, is called a *benefit-only* pattern and is ascribed to automatic facilitation (AF).

In contrast, for long RSIs, first-order alternations are faster than repetitions, and higher-order effects are more complicated. For example, after a sequence of 1's, the subject's response to another 1 is faster, while the response to a 2 is slower. Following the alternating sequence 1-2-1-2-1, the response is faster to a 2 and slower to a 1. This cost-benefit phenomenon is believed to be caused by strategic expectancy (SE; previously called subjective expectancy; see Bertelson, 1961; Laming, 1968; Kirby, 1976). It implies that RTs tend to be shorter if the current stimulus confirms the subject's expectation and longer otherwise. Expectation of a pattern even if the sequence is random is also known as the gambler's fallacy (Jarvik, 1951; Tversky & Kahneman, 1974).

The transition from AF to SE occurs at a critical response-to-stimulus interval (RSI) above 100 ms, although the value differs significantly from

experiment to experiment. For example, Cho et al. (2002) reported sequential effects dominated by first-order AF and higher-order SE for RSI = 800 ms. Relative strengths of AF and SE are also affected by practice and stimulus-response compatibility; specifically, practice weakens AF more than it does SE (Soetens et al., 1985), and with an incompatible stimulus-response mapping, the transition from AF to SE occurs later (at 250–500 ms RSI) (Soetens et al., 1985; Jentzsch & Sommer, 2002).

Although no SE effect has been explicitly shown in RTs or ERs at short RSIs, some neurophysiological data do provide evidence of expectancy. An electroencephalogram (EEG) study (Sommer et al., 1999) shows a clear sequential effect with an SE pattern in the P300 response, an event-related potential (ERP) component peaking at approximately 300 ms after stimulus onset, under both long (500 ms) and short (40 ms) RSIs (for longer RSIs, the amplitude is much larger). Further studies also identify specific components of P300 that are sensitive to sequential effects (Jentzsch & Sommer, 2001, 2002), although more detailed studies are needed to be conclusive.

Sequence-related activity has been observed in the prefrontal cortex (PFC), among other areas. In particular, Huettel, Song, and McCarthy (2005) demonstrated PFC activation after sequence violation and found that activation levels increase as the sequence preceding violation lengthens. (Subregions of PFC that are most sensitive to specific sequence patterns were also identified, although the time resolution is too low to reveal dynamical details.) This provides evidence that "higher-order" brain regions can develop expectancy by accumulating memory of past trials and register violations when an expected pattern fails to appear.

Previous modeling studies (Squires, Wickens, Squires, & Donchin, 1976; Soetens, Deboeck, & Hueting, 1984; Cho et al., 2002; Jones, Cho, Nystrom, Cohen, & Braver, 2002) have succeeded in matching specific experimental observations, but none has addressed sequential effects over a wide range of RSIs as in the experiment of Soetens et al. (1985) or attempted to explain sequential effects in different experiments or elucidate their neural mechanisms. Building on an established connectionist model of decision making (Usher & McClelland, 2001), this article addresses this omission by implementing three biasing mechanisms: residual activity from the immediately previous trial that influences the initial condition in the current trial, expectation-based top-down bias, and bias due to conflict monitoring. Before combining these mechanisms to match various data, we separate them in order to probe their individual effects and explore which mechanisms are most critical to particular observations. We find that varied transitions from AF to SE under different experimental conditions can be explained by different timescales in decision-layer dynamics and that speeding up all the mechanisms can account for changes in RT patterns due to practice.

We follow traditional use, taking automatic facilitation (AF) to refer to faster responses to repetitions (in first-order AF) and the benefit-only

pattern in RTs (higher-order AF), and strategic expectancy (SE) to refer to faster responses to alternations (first-order SE) and the cost-benefit pattern (higher-order SE). Similar terms are used in the discussion of sequential effects in error rates and neural activities.

This article is organized as follows. In section 2, we introduce the connectionist network and augment it in section 2.1.2 with a model for residual activity due to previous trials. Sections 2.1.3 to 2.1.4 develop detailed top-down biasing mechanisms related to expectancy and conflict monitoring, and two models of the biasing effects are advanced for the latter. Simulation methods and parameter choices are reviewed in section 2.2. Predictions of the models are then described in section 3, in which we investigate the effects of each mechanism individually. We show in section 3.1.1 that residual activity alone cannot produce higher-order AF and in sections 3.1.2 and 3.1.3 that higher-order AF and SE behavioral effects are accounted for by top-down biasing mechanisms. We focus on sequential effects on reaction times in this article but briefly address the effects of noise on error rates in section 3.1.4. The effects of the combined biases are presented in sections 3.2 to 3.3, where we also address the effects of practice. In section 4, we summarize, note some open questions, and comment on possible neural mechanisms.

2 Methods

In this section we develop a basic mathematical model that encompasses decision dynamics and propose biasing mechanisms that account for AF and SE effects. We start by briefly reviewing the leaky competing accumulator model and then, drawing on preliminary analyses of its behavior and on prior work, propose adjustments to initial conditions and input currents to the accumulators based on prior responses.

2.1 A Computational Model of Decision Making with Biasing Mechanisms. Figure 1A summarizes the overall model architecture. Stimulus inputs feed to a decision layer containing competing neural units that race toward a decision criterion or threshold (see Figure 1B). The current trial's status as a repetition or alternation is combined with that of previous trials in short-term memory modules (green and yellow units). Response conflict over recent trials is similarly maintained as in the conflict-based mechanism of Botvinick, Braver, Barch, Carter, and Cohen (2001) (brown unit). We extend that work by incorporating temporal dynamics in the biasing mechanisms during RSI. These "higher" modules then influence the decision or sensory layers in subsequent trials by excitatory or inhibitory feedback. We also include the effects of decaying neural activity after reaching threshold (see Figure 1C), as revealed in both experiments and modeling (e.g., Roitman & Shadlen, 2002; Lo & Wang, 2006).

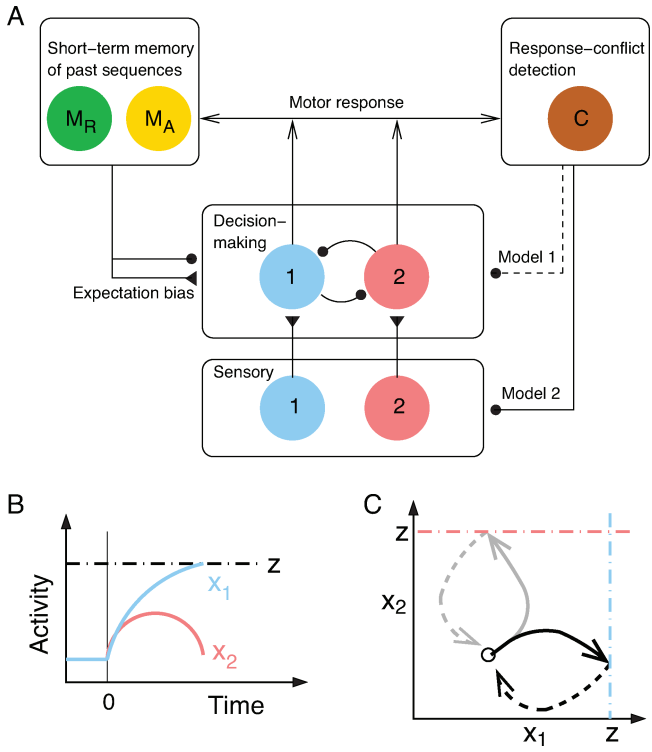

Figure 1: Schematic diagram of the models and neural dynamics during decision making. (A) Sensory-layer outputs enter a decision-making layer containing competing, mutually inhibited units that accumulate evidence for choices 1 and 2. Biasing modules temporarily store memories of past repetition (M_R) or alternation (M_A) sequences, and response conflict (C) during evidence accumulation. Filled triangles (circles): excitatory (inhibitory) connections. Inhibition on decision units (model 1) or sensory units (model 2) depends on conflict level (see the text for details). (B) Time course of neural activities in decision layer after stimulus onset at time 0: here choice 1 is made, and z denotes the decision threshold (dash-dotted). (C) Representation of neural dynamics on the two-dimensional decision space. Solid black (gray) curves starting at the circle denote trajectories of neural dynamics with x_1 (x_2) winning, and dashed lines show post-decision trajectories; thresholds shown dash-dotted.

2.1.1 Decision Layer Model. We employ the connectionist model of Usher and McClelland (2001), in which the activaties $x_1(t)$, $x_2(t)$ of two decision units are described by stochastic differential equations coupled by mutual inhibition (see Figure 1A). Each unit has overall time constant τ_c, a passive leakage term of strength k, an input ρ_i representing the stimulus, and an independent and identically distributed gaussian noise process η_i. Inhibition

of strength β acts via a sigmoidal function $f(x_i) = 1/[1 + \exp(-G(x_i - d))]$, where G is the gain and d is a half-activity offset:

$$\tau_c \frac{dx_1}{dt} = -kx_1 - \beta f(x_2) + \rho_1 + \sigma\eta_1(t), \tag{2.1a}$$

$$\tau_c \frac{dx_2}{dt} = -kx_2 - \beta f(x_1) + \rho_2 + \sigma\eta_2(t). \tag{2.1b}$$

This formulation is equivalent to a firing rate model via a linear transformation (Grossberg, 1988; Brown et al., 2005), and reductions to one-dimensional drift diffusion and Ornstein-Uhlenbeck systems can be made in appropriate parameter ranges (Brown & Holmes, 2001; Bogacz, Brown, Moehlis, Holmes, & Cohen, 2006).

Under the free response protocol, a decision is made when either unit first reaches a preset activity threshold $x_i = z$. The decision time is the time taken for that unit's state to reach threshold from its initial condition. Model 2.1a and 2.1b captures a variety of experimental observations, is neurophysiologically plausible, and offers a framework to which representations of other brain areas can be added (Botvinick et al., 2001). In particular, it has previously been used to model sequential effects (Cho et al., 2002). Unless otherwise noted, we henceforth adopt the parameters in Cho et al. (2002) and Usher and McClelland (2001): $\tau_c = 0.1$, $k = 0.2$, $\beta = 0.75$, $G = 4$, $d = 0.5$, $\rho_0 = 0.35$, $z = 1.05$, setting $\rho_i = 0.5 + \rho_0$ when stimulus i is shown and $\rho_i = 0.5 - \rho_0$ when it is not. Here ρ_0 is the stimulus sensitivity, which may differ in different situations even for the same subject and same stimulus. Further comments on τ_c appear in section 2.2.

2.1.2 Post-response Residual Activity. Physiological studies such as Roitman and Shadlen (2002) show that neurons that accumulate evidence during decision tasks experience rapid decay, or inhibitory suppression, of activity following responses (see Lo & Wang, 2006, for a related modeling study). The amount by which activities decay in equations 2.1 during the RSI can influence the following trial by changing the initial condition before integration begins (see Figure 1C).

The analysis in section 3.1.1 and the supplementary materials[1] shows that activities $x_i(t)$ decay from their states at the previous response toward a stable fixed point. As shown there, several manipulations have been tried to match typical RTs in Soetens et al. (1985), one of which is to increase the leak and inhibition parameters during RSI. This mechanism, consistent with findings of Roitman and Shadlen (2002), effectively applies global inhibition during RSI to reset the accumulators more rapidly. Using the values $k = 4$

[1]Supplementary materials are available online at http://www.mitpressjournals.org/doi/suppl/10.1162/neco.2009.09-08-866.

and $\beta = 15$ throughout the RSI, we find that apart from a brief (< 50 ms) postresponse transient in which the losing unit on the last trial decays, the resulting initial conditions can be approximated by

$$x_{i0} = 0.5ze^{-\frac{RSI}{\tau_x}} + \bar{x} \quad \text{and} \quad x_{j0} = -1.5ze^{\frac{RSI}{\tau_x}} + \bar{x}. \tag{2.2}$$

Here $x_1 = x_2 = \bar{x}$ is the intertrial equilibrium state, unit i is the winner, unit j the loser, z the decision threshold, and the timescale $\tau_x = 50$ ms. This provides a simplified description of residual activity that will be used below, along with biases due to response conflict and expectation.

2.1.3 Biases from Expectations. We assume that strength of expectation is determined by memory of the previous sequence with more recent trials playing a more important role. Specifically we define memories of repetition and alternation over trials as follows:

$$M_R(n) = \Delta_R M_R(n-1) + I_R(n-1), \tag{2.3a}$$

$$M_A(n) = \Delta_A M_A(n-1) + I_A(n-1), \tag{2.3b}$$

where

$$I_R(n-1) = \begin{cases} 1, & \text{if } S(n-1) = S(n-2), \\ 0, & \text{otherwise;} \end{cases} \tag{2.4a}$$

$$I_A(n-1) = \begin{cases} 0, & \text{if } S(n-1) = S(n-2), \\ 1, & \text{otherwise,} \end{cases} \tag{2.4b}$$

and $S(n-j)$ is the stimulus in the $(n-j)$th trial. Similar definitions appeared in Cho et al. (2002).

The discrete linear mapping of equations 2.3 and 2.4 is equivalent to a low-pass filter with timescale $1/(1-\Delta)$, where $\Delta = \Delta_R$ or Δ_A is a constant in the range from 0 to 1. The process mimics decaying memories of alternation and repetition in the stimulus history and can also be interpreted as computing time-discounted fractions of alternations and repetitions. Control biases from higher-level units, assumed proportional to the memories of alternation M_A or repetition M_R, will be used to bias the nth trial (cf. Figure 1A).

Huettel, Mack, and McCarthy (2002) show that cross-trial dynamics approach saturation after a shorter sequence of repetitions relative to alternations, implying a faster decay rate for repetitions: $\Delta_R < \Delta_A$. This is true on both neural and psychometric levels, as confirmed by reanalysis of RTs from Cho et al. (2002) and Soetens et al. (1985) (see Figure 2). Consistent with this, we set $\Delta_R = 0.4$ and $\Delta_A = 0.6$, retaining the mean value 0.5 used in Cho et al. (2002).

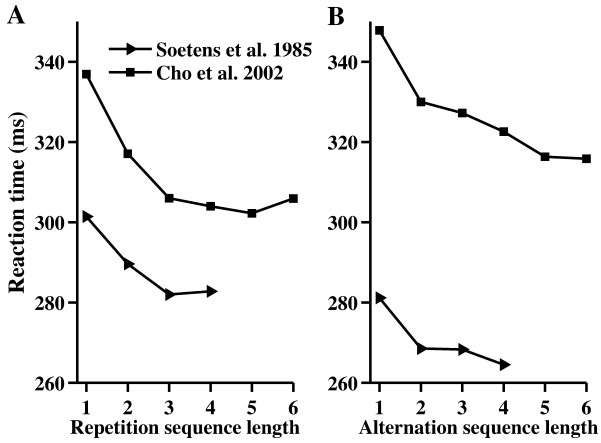

Figure 2: Different decay rates for continuation of repetitions and alternations. Effects of pure repetition (A) saturate after shorter sequences than those of pure alternation (B), as shown by reanalysis of mean RT data in Cho et al. (2002) and Soetens et al. (1985), with authors' permissions. Data identified by key.

Figure 2 illustrates two further facts: (1) mean RTs in Cho et al. (2002) (squares) are longer than those in Soetens et al. (1985) (triangles); and (2) repetitions are faster in the former, although RSIs are long for both data sets (800 ms and 1000 ms, respectively). We believe the first is because the task in Cho et al. (2002)—discrimination between capital and lowercase o's—is harder than detecting lighted LEDs as in Soetens et al. (1985). The second fact, to be addressed in section 3, provides evidence of first-order AF and higher-order SE in the data for an 800 ms RSI, contrary to the prior suggestion of a critical transition at 100 ms RSI (Soetens et al., 1985).

Short-term memories for repetition and alternation are assumed to work independently and in parallel as in Cho et al. (2002), and we assume a linear relationship between memory and biasing strength $B_{i,n}$ at the nth trial:

$$B_{i,n} = \gamma_B M_i(n), \text{ where } i = \text{R or A}, \tag{2.5}$$

where M_R and M_A are the repetition and alternation memories of equations 2.3 and γ_B is set to 0.1 throughout. We additionally assume that the biasing strength grows over time before each trial following the delayed exponential equation:

$$b_{i,n}(RSI) = \begin{cases} B_{i,n}\left[1 - \exp\left(-\frac{RSI - T_0}{\tau}\right)\right], & \text{if RSI} > T_0, \\ 0, & \text{otherwise.} \end{cases} \tag{2.6}$$

This implements the intuition that time is needed for the cortex to initiate top-down control. The neurophysiological data of Sommer et al. (1999) indicate that SE-related neural activity occurs for RSIs as low as 40 ms, but with amplitudes smaller than those for long RSIs. Guided by this, we selected a latency of $T_0 = 30$ ms to allow AF to dominate for very short RSIs. In the supplementary materials, it is shown that the resulting model adequately reproduces observed P300 neural activity patterns thought to be related to expectation. A sigmoidal rise in $b_{i,n}$ with RSI could also capture delayed growth, and such a smooth function, also specifiable by two parameters, may derive more naturally from neural dynamics, although we do not expect the precise form to affect our results.

We further suppose that after longer sequences of repetitions or alternations, subjects need less time to develop expectations for the coming trial; hence, PFC activity develops more rapidly during the RSI in these cases. This is modeled by letting the timescale τ in equation 2.6 depend linearly on memory $M_i(n)$ or, equivalently, on the saturation value $B_{i,n}$. Specifically, τ attains a maximum $\tau = \tau_0 \approx 600$ ms for $B_{i,n} = 0$ and approaching $\tau = 0$ after an infinite sequence: $\tau = \tau_0(1 - B_{i,n}/\hat{B})$, where $\hat{B} = 0.25$ is the maximum values $\gamma_B \hat{M}_i$ achieved after arbitrarily long strings of R's or A's. The final update rule is therefore

$$b_{i,n}(RSI) = \begin{cases} B_{i,n}\left[1 - \exp\left(-\frac{RSI - T_0}{\tau_0(1 - B_{i,n}/\hat{B})}\right)\right], & \text{if RSI} > T_0 \\ 0, & \text{otherwise} \end{cases}. \tag{2.7}$$

This development of expectation-related bias $b_{i,n}$ during RSI following each trial can be approximated by a linear leaky integrator equation,

$$\frac{db_i}{dt} = -\frac{1}{\tau} b_i + \alpha B_i, \quad \text{where} \quad i = \text{R or A},$$

and α is a scaling constant. The decrease in τ for larger B_i can result from a saturation factor, as in

$$\frac{db_i}{dt} = -\frac{b_i}{\tau} + (1 - b_i)\alpha B_i \quad \Rightarrow \quad \frac{db_i}{dt} = -\frac{1}{\tau_e} b_i + \alpha B_i, \tag{2.8}$$

where $\tau_e = \tau/(1 + \alpha B_i \tau)$, implying smaller τ_e for larger B_i. Equation 2.8 has the same form as the dynamical equation for a saturating synaptic gating variable, such as NMDA-mediated receptors, which have been used in biophysical modeling of prefrontal cortical microcircuits (Wang, 1999).

We assume that the biases stop increasing when the next stimulus appears and remain fixed for its duration, much as short-term memories can be maintained by line attractors (Seung, 1996; Machens, Romo, & Brody, 2005). If biases continued increasing regardless of stimulus onset, they would

saturate even for short RSIs, and sequence-related neural activities would be similar for both short and long RSIs, provided that the overall RT plus RSI duration is sufficient. This conflicts with the finding in Sommer et al. (1999) that $P300$ activity is significantly lower for short RSIs. Truncation of the development of neural activity can be understood as occurring when attention shifts to the stimulus at trial onset, establishing persistent activity in the PFC, or as due to saturation of synapses (cf. equation 2.8).

Finally, the top-down control mechanisms that mediate expectation are assumed to send excitatory bias $+B_{i,n}$ to the decision unit that would confirm the expectation and inhibitory bias $-B_{i,n}$ to the one that violates it. Thus, for previous stimulus 1, in the next trial, expectation of repetition sends positive bias to unit 1 and negative bias to unit 2, whereas expectation of alternation sends positive bias to 2 and negative bias to 1. Bias is added to the input currents representing the stimuli, so that the dynamics of the nth trial with expectation-related bias alone is given by

$$\tau_c \frac{dx_1}{dt} = -kx_1 - \beta f(x_2) + \rho_1 + b_{R,n}(RSI) - b_{A,n}(RSI) + \sigma\eta_1, \tag{2.9a}$$

$$\tau_c \frac{dx_2}{dt} = -kx_2 - \beta f(x_1) + \rho_2 - b_{R,n}(RSI) + b_{A,n}(RSI) + \sigma\eta_2. \tag{2.9b}$$

2.1.4 Biases Due to Response Conflict Monitoring. It has long been recognized that conflict is an important feature of cognitive processing (e.g., Berlyne, 1960), and computational modeling work has suggested that response conflict monitoring mechanisms may play an important role in signaling the need for cognitive control (Botvinick et al., 2001).[2]

In connectionist networks, conflict is typically quantified as the integrated product of activities in the competing decision units:

$$E_n = \int_{trial} f(x_1(t))\, f(x_2(t))\, dt, \tag{2.10}$$

implying that high conflict follows trials in which both units are active and decision times are long. This formulation of strategic priming was introduced in Botvinick et al. (2001) and Jones et al. (2002) via the updating rule

$$C_n = \lambda C_{n-1} + (1-\lambda)\alpha E_{n-1}, \tag{2.11}$$

in which the decay rate λ lies between 0 and 1, and $\alpha < 0$ denotes inhibitory bias. Note that conflict C_n in the nth trial does not affect that trial but

[2]Some aspects of this view have recently been questioned (Burle, Allain, Vidal, & Hasbroucq, 2005; Burle, Roger, Allain, Vidal, & Hasbroucq, 2008).

influences the $(n+1)$st trial. Considering residual activities, it follows from equations 2.1 to 2.2 and 2.10 to 2.11 that if each decision unit is alternately stimulated (alternating trials), conflict levels will be higher than the case where only one is active (repetition trials).

Direct calculations using equations 2.10 and 2.11 and the parameters of Botvinick et al. (2001) and Jones et al. (2002) reveal that strategic priming strengths decrease as RSIs increase, because neural activities have more time to decay for longer RSIs, producing lower conflict levels. Plotting priming strengths versus different RSI values reveals almost perfect exponential decay during RSI, the timescale of which depends on priming strength in an approximately linear manner. (See the supplementary materials for details.)

Motivated by these observations, we simplify the conflict-based biasing mechanism as follows. Noting that adding the same amount of conflict in all conditions does not change sequential effect patterns, we assume that conflict monitoring is engaged only following alternations. Rather than compute the integral, equation 2.10, after each trial, we parallel the discrete formulation of equation 2.5 by modeling inhibition due to strategic priming during the nth trial as

$$p_n(RSI) = -P_n e^{-\frac{RSI}{\tau_p}}, \tag{2.12}$$

where the minus sign means it is inhibitory and P_n is the predecay priming strength at the previous response whose value is proportional to the prior alternation content in the stimulus sequence:

$$P_n = \gamma_P M_A(n), \tag{2.13}$$

with $\gamma_P = 0.3$ throughout and $M_A(n)$ being the alternation memory after the $(n-1)$st response (cf. equation 2.3b). The time constant in equation 2.12 is allowed to depend linearly on the predecay strategic priming strength P_n via $\tau_p = \tau_{p0} - \kappa P_n$, and we take $\tau_{p0} = 0.5$, $\kappa = 0.4$, to place τ_p in the appropriate range of 200 to 500 ms to yield reasonable RTs.

Summarizing, equations 2.12 and 2.13 imply that conflict-mediated bias during the nth trial is given by

$$p_n(RSI) = -P_n e^{-\left(\frac{RSI}{\tau_{p0}-\kappa P_n}\right)}. \tag{2.14}$$

The supplementary materials show that this simplified conflict-monitoring mechanism resembles the original one of Jones et al. (2002) and Botvinick et al. (2001) and however, it also enables the separation of this mechanism from others and allows an explicit examination of its strengths and effects as RSI varies (see section 3.1.3). Although several studies (Jones et al.,

2002; Jentzsch & Leuthold, 2005; Soetens & Notebaert, 2005) suggested that higher-order AF may be due to conflict monitoring following task execution, they did not explicitly address the effects on reaction times and error rates for different RSI values.

We propose two different implementations for top-down cognitive control. In model 1, response conflict decreases the inputs to both decision units by adding equal inhibitory biases to them (see Figure 1A). As in similar models of conflict-mediated control (Botvinick et al., 2001; Jones et al., 2002), we include baseline activity by adding a constant p_{base} ($= 0.5$ here, as in Jones et al., 2002) so that inputs remain in the same range. With this mechanism alone, the dynamics during the nth trial are governed by

$$\tau_c \frac{dx_1}{dt} = -kx_1 - \beta f(x_2) + \rho_1 + p_n(RSI) + p_{\text{base}} + \sigma\eta_1, \tag{2.15a}$$

$$\tau_c \frac{dx_2}{dt} = -kx_2 - \beta f(x_1) + \rho_2 + p_n(RSI) + p_{\text{base}} + \sigma\eta_2. \tag{2.15b}$$

Alternatively, in model 2, we suppose that response conflict decreases the sensitivity to stimuli. Instead of the symmetric bias $\rho_j \mapsto \rho_j + p_n(RSI)$, we reset stimulus sensitivity $\rho_0 \mapsto \rho_0 + p_n(RSI)$. Since $p_n(RSI) < 0$, this decreases the difference $|\rho_1 - \rho_2| = 2\rho_0$ between the inputs. Similar to the addition of baseline activity in the first implementation, we add baseline sensitivity $\rho_0 \mapsto \rho_0 + p_n(RSI) + 0.15$ such that the resulting new ρ_0 values fall into a reasonable range. With this acting alone, the resulting RTs also exhibit a typical AF pattern. (See Figure 5, bottom.) To keep ρ_0 positive, we set $\gamma_P = 0.15$.

Testing them in combination with the other mechanisms developed above, we shall see in sections 3.1.4 and 3.2 that while both capture sequential effects on reaction times, model 2 produces more realistic error rates.

2.2 Parameters, Simulation Methods, and Inclusion of Noise. In Table 1, we summarize the complete parameter set introduced above and specify the values used in the simulations of section 3. Many of these are taken directly from previous modeling work, and none is entirely free.

For numerical simulations of equations 2.1, we employ the Euler-Maruyama method (Higham, 2001). The behavioral RT comprises the decision time (DT) and a nondecision-related latency (T_{sm}) that includes sensory processing and motion execution (Usher & McClelland, 2001; Shadlen & Newsome, 2001). We set RT $= DT + T_{sm}$ where $DT = \tau_c N_c$ and N_c is the number of steps required to simulate one trial. Note that τ_c also appears in equations 2.1: smaller τ_c implies quicker decay and larger inhibition. We set $\tau_c = 0.1$ throughout to be in general agreement with Cho et al. (2002) and use step size $dt = 0.02$, so that each simulation step corresponds to 2 ms in real time. We fix $T_{sm} = 160$ ms, putting RTs in the same range

Table 1: Parameter Values for the Models.

Decision Layer Parameters

Parameter	Value	Notes	Parameter	Value	Notes
k	0.2	Adopted from U01/C02	β	0.75	Adopted from U01/C02.
ρ_0	0.35	Adopted from U01/C02	z	1.05	Adopted from U01/C02.
G	4	Adopted from U01/C02	d	0.5	Adopted from U01/C02.
τ_c	0.1	Consistent with C02	T_{sm}	160 ms*	Consistent with U01.

Biasing Mechanism Parameters

Parameter	Value Model 1	Value Model 2	Notes
τ_x	50 ms*	-	Equation 2.2. From connectionist model.
Δ_R	0.4	-	Figure 2. Consistent with C02/S85.
Δ_A	0.6	-	Figure 2. Consistent with C02/S85.
T_0	30 ms	-	Consistent with S99 and S85.
γ_B	0.1	-	To match S85
τ_0	600 ms*	-	Equation 2.7. To match S85
γ_p	0.3	0.15	To match S85.
τ_{p0}	500 ms*	-	Equation 2.14. Consistent with
κ	0.4	-	J02/B01 and to match S85.
p_{base}	0.5	0.15	Adopted from J02 for Model 1; to match S85 for Model 2.

Notes: Works cited are abbreviated as follows. U01: Usher and McClelland (2001); C02: Cho et al. (2002); S85: Soetens et al. (1985); S99: Sommer et al. (1999); J02: Jones et al. (2002); B01: Botvinick et al. (2001). Asterisks indicate that different values were used to match specific data in section 3.3; dashes in column 3 of the biasing mechanism parameters indicate that values are the same for both conflict-biasing models.

as the data of Soetens et al. (1985), which is consistent with the literature (cf. Usher & McClelland, 2001). The value of T_{sm} does not affect the pattern of sequential effects (it simply changes absolute RT values), and the value of τ_c does not affect our qualitative conclusions (it uniformly changes the slopes of the curves in Figure 7).

Due to the relative lack of data on error rates, we focus on sequential effects on RTs under changes of RSI, initially ignoring noise by setting $\sigma \equiv 0$ in equations 2.1, and asking how different deterministic mechanisms individually affect RTs. We show that the resulting reaction time patterns are unaffected by moderate noise and then devote a short section to sequential effects on ERs. In the final simulations, gaussian noise with standard deviations $\sigma = 0.3$ for the first model and $\sigma = 0.4$ for the second model is introduced in order to produce appropriate error rates (see Figure 7, bottom panels).

Our primary goal is to propose mechanisms that qualitatively reproduce previous data and offer explanations for the various effects, so we do not perform parameter fits to specific experiments. Nonetheless, as noted in Table 1, model parameters are adapted from or chosen consistent with previous work and to yield reasonable RTs and ERs, and we include comparisons with data from Soetens et al. (1985), Kirby (1972), Vervaeck and Boer (1980), and Cho et al. (2002).

3 Results

In this section, we repeatedly use two graphical devices that have been developed to display the influence of sequential effects: RT versus stimulus sequence graphs and repetition-alternation scattergraphs. The former describe sequential effects on decision performance by plotting mean RTs or ERs for different sequence histories as in Figure 7 below (cf. Soetens et al., 1985, Fig. 2). Points on the abscissa denote the 2^N possible sequences of length N, and the ordinates are the corresponding mean RTs (or ERs) for the last trial in the sequence (the bottom entry). The data divide into a repetition curve on the left (the last trial is R) and an alternation curve on the right (the last trial is A). First-order effects adjust the relative positions of the repetition and alternation curves; higher-order effects influence their relative slopes.

The repetition-alternation scattergraph or exchange function was introduced in Audley (1973) (see Figure 8 below; cf. Soetens et al., 1985, Fig. 1). Each point represents a given prior sequence (e.g., ARA), its abscissa being the mean RT of repetition trials following that sequence ($ARAR$) and its ordinate the mean RT of subsequent alternation trials ($ARAA$). Points aligned at approximately 45 degrees correspond to a pure AF effect, meaning that certain sequences lead to shorter RTs and others lead to longer RTs, regardless of how they continue. In contrast, an angle of approximately -45 degrees identifies a pure SE pattern, implying that if a sequence leads to shorter

RTs under continued repetition, it yields a longer RT for an alternation and vice versa. Thus, plotted versus RSI as in Figure 9 below, the angle of the repetition-alternation scattergraph changes from positive to negative as RSI increases and AF transitions to SE (cf. Soetens et al., 1985, Fig. 5).

3.1 Effects of Individual Biasing Mechanisms on Mean Reaction Times. We first examine how the different biasing mechanisms individually influence decision RTs and ERs, following the order of their introduction in section 2. We then present simulation results on reaction times and error rates that combine the three strategies of sections 2.1.2 to 2.1.4.

3.1.1 Residual Activity Does Not Cause Higher-Order Facilitation. Conventionally, both first- and higher-order AF are ascribed to residual traces of previous stimuli that accumulate across trials, leading to facilitation at short RSIs (Soetens et al., 1984, 1985). Contrary to this, we show here that simulations of equation 2.1 with only decay of unit activities during RSI suggest that the characteristic positive slope of the alternation curve cannot be explained by residual activity in the decision layer alone.

The top panel of Figure 3 shows residual activities remaining from previous trials that form initial conditions $x_i(0)$ for the current trial. Current stimuli are always assumed to be 1. Thus, in repetition curves, the previous stimulus was also 1, whereas in alternation curves, it was 2. Here we adopt the parameters of section 2.1.1 during stimulus presentation but increase leak and inhibition to $k = 4$ and $\beta = 15$ during RSI, preserving the ratio $\beta/k = 3.75$. As explained in the supplementary materials, residual unit activities that remain following the decay of states in the absence of stimuli during RSI form initial conditions for the next trial. The resulting dependence of initial conditions on RSI, shown in supplementary Figure 4, suggests the simplified residual activity description of section 2.1.2.

The repetition RT curves are all flat (left-hand side of Figure 3B), although the residual activities are not (lowest curve on left-hand side of Figure 3A). By expressing the history sequences in terms of 1 and 2, one can see that alternation RT curves can have only negative slope, although this is evident only for the shortest RSIs. For example, $RRRA$ and $RAAA$ correspond to 22221 and 22121, assuming the current stimulus is 1. Unit 1 is evidently at a greater disadvantage at the beginning of the current trial for $RRRA$ than for $RAAA$, leading to a larger RT for $RRRA$. The resulting negative slope of the alternation curves implies that higher-order facilitation is not due to dynamics within the decision layer alone but rather to top-down mechanisms.

3.1.2 Expectation Bias Changes Slopes of Repetition and Alternation Curves in Opposite Ways. Expectation-based biases produce the opposite-sign slopes in repetition and alternation RT curves characteristic of SE, as shown in Figure 4. This pattern becomes clearer as RSI increases due to the

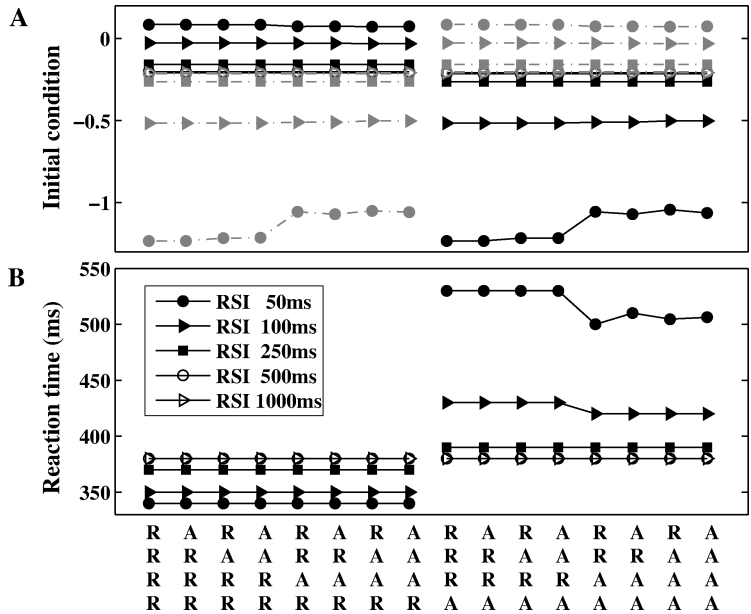

Figure 3: Residual activity shifts RTs vertically. (A) Initial conditions of units 1 (solid black) and 2 (dashed gray) after sequence histories shown in abcissa, with current stimulus 1. The previously winning unit starts closer to threshold on repetition curve and farther from threshold on alternation curve for all RSIs (results coincide at ≈ -0.2 for RSI 500 and 1000 ms). (B) RT curves shift vertically as RSI varies but remain predominantly horizontal, repetitions being faster than alternations for all RSIs. Parameters are as in Usher and McClelland (2001), except for decay rate $k = 4$ and inhibition strength $\beta = 15$ during RSI. See the key for symbols denoting RSIs.

development of expectation and bias over time. Since only the relative bias to the two units influences sequential effects, other strategies can yield similar results (e.g., if only one unit is biased with parameter γ_B suitably increased). Note that the repetition and alternation curves are not horizontal for RSI $= 50$ ms; instead, both are kinked: at *AAAR* in the repetition curve and at *AAAA* in the alternation curve. This is because the expectation timescale is faster after longer sequences, which is important in capturing the breakthrough phenomenon, explained in section 3.2.

3.1.3 Conflict-Based Bias Can Cause Higher-Order Facilitation. Since alternations result in higher conflict, biasing the decision layer by response conflict from previous trials leads to greater effects as the proportion of alternations in the sequence grows (see the top panel of Figure 5), although the overall effect weakens as RSI lengthens, due to decaying bias

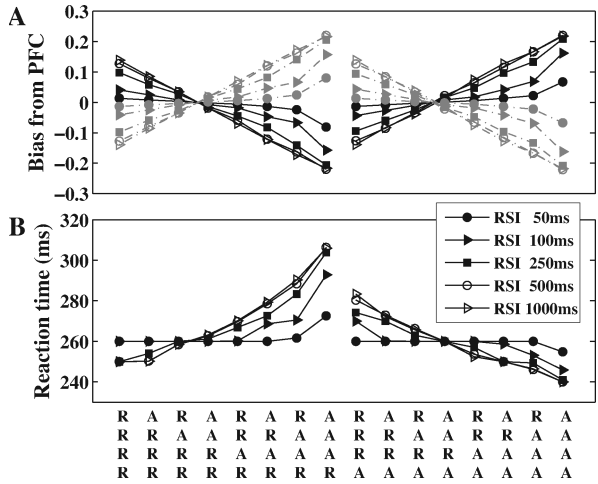

Figure 4: Expectation biases RT slopes asymmetrically. (A) Biases from expectation-related neural activity to unit 1 (solid black) and 2 (dashed gray), assuming current stimulus is 1. Since biases to the decision units are opposite in sign, opposite changes in slope occur for repetition and alternation curves as RSI varies. (B) Mean RTs resulting from this mechanism alone: as RSI decreases, slopes decrease. See the key for symbols denoting RSIs.

(see equation 2.14). The resulting RTs exhibit a parallel slope AF pattern, which becomes less sequence dependent as RSIs increase. This trend is similar whether inhibition is sent to the decision layer (model 1) or the sensory layer (model 2): Figure 5 (center, bottom). Thus, higher-order facilitation can derive solely from conflict-based inhibition.

3.1.4 Effects of Noise on Error Rates. When white noise is included in equations 2.1, the basic RT patterns described above persist, and each feedback mechanism produces a characteristic error pattern, as shown in Figure 6. Since less experimental data are available to reveal the dependence of ERs on RSI, we collapse the five RSI conditions to two: short (RSI = 50 and 100 ms) and long (RSI = 250, 500, and 1000 ms), as in Soetens et al. (1985).

The major effects are as follows. Residual activities produce approximately uniform ERs for long RSIs but alternation ERs are notably higher and repetition ERs lower for short RSIs (top left), and the expectation bias is reflected in the overall positive and negative ER slopes of the repetition and alternation curves, respectively (top right). RT patterns are similar for both conflict models (see Figure 5), but model 2 predicts more realistic ER patterns with higher ERs for short RSIs (bottom right) while model 1 reverses this and produces lower ERs overall (bottom left), and the general trends of slopes for short RSIs are also reversed.

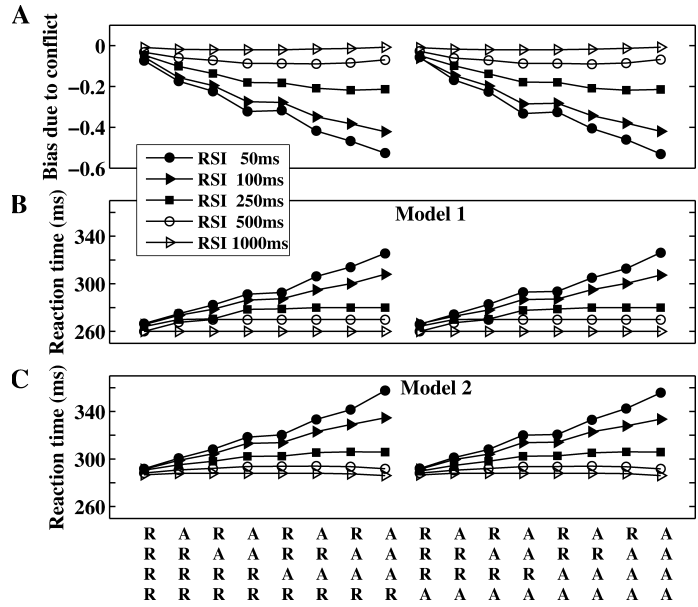

Figure 5: Conflict bias produces parallel RT slopes. (A) Biases $p_n(RSI)$ to neural units 1 and 2 due to response conflict, assuming current stimulus is 1. Repetition and alternation curves are identical, since both units receive the same bias. (B) Mean RTs resulting from the first implementation alone: as RSI decreases, slopes increase as curves rotate counterclockwise about their left-hand ends. (C) Mean RTs resulting from the second implementation alone. See the key for symbols denoting RSIs.

3.2 Combined Biasing Mechanisms Account for Reaction Times and Error Rates. We now combine the residual activity model of section 2.1.2, bias derived from the expectation-mediated top-down control mechanism of section 2.1.3 and the response conflict biasing mechanisms (model 1 or 2) of section 2.1.4. Both versions of the complete model can reproduce sequential effects on RTs over the range of RSIs examined in Soetens et al. (1985). Specifically, the upper panels of Figure 7 show that (1) as RSIs increase, the position of the alternation curve shifts from above to below that of the corresponding repetition curve, and (2) its overall slope changes from positive to negative with the transition from AF to SE occurring when RSI reaches ≈ 100 ms. Finally (3), breakthrough occurs. This is signaled by a strong decrease in mean RT in passing from *RAAA* to *AAAA* and a strong increase in RT between *RAAR* and *AAAR* at short RSIs.

Breakthrough is robustly observed in almost all experiments (Soetens et al., 1984, 1985; Sommer et al., 1999), although its size varies, being influenced by factors such as practice and aging (Vervaeck & Boer, 1980; Melis, Soetens, & van der Molen, 2001). If AF alone dominated at short RSIs, mean

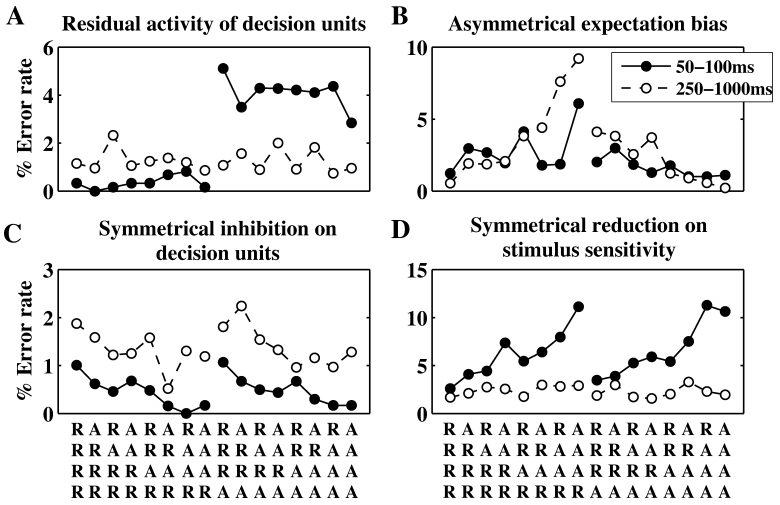

Figure 6: Error rates resulting from added noise. Each panel shows the effect of one mechanism. (A) Residual activity. (B) Expectation bias. (C) Conflict bias, the first implementation. (D) Conflict bias, the second implementation. Averages performed over 5000 trials with white noise of standard deviation 0.5. Note the differences in vertical scales.

RTs should be longer after three than after two alternations, even if the current trial is also an alternation. However, the fact that RTs for *AAAA* are shorter than for *RAAA* implies that SE operates at very short RSIs in breakthrough and that a critical number of alternations is required for subjects to detect a pattern and form an expectation for the coming trial. The model produces these effects by allowing the timescales τ and τ_P to depend on sequence lengths (see equations 2.6–2.7, and 2.12 and 2.14).

The error rates of Figure 7 show that both conflict bias models capture the qualitative ER pattern at long RSIs but that model 1 fails for short RSIs, predicting an alternation curve with negative slope in contrast to the positive slope exhibited in Soetens et al. (1985).

To compare with Figure 1 of Soetens et al. (1985), we show repetition-alternation scattergraphs in Figure 8 and their slopes in Figure 9. Also compared are data from Kirby (1972) and Vervaeck and Boer (1980). In computing slopes by linear regression, the breakthrough points (*AAAR* and *AAAA*) are excluded. As expected, slopes decrease with increasing RSI, passing through zero around 100 ms, as concluded in Soetens et al. (1985). Slopes derived from the data of Soetens et al. (1985) using the same regression algorithm are also shown in Figure 9 for comparison. Both data and model results exhibit similar negative (positive) slopes for long (short) RSIs. We emphasize that RTs collected in different experiments can differ substantially, as shown in Figure 8 (bottom panels); here we focus on general

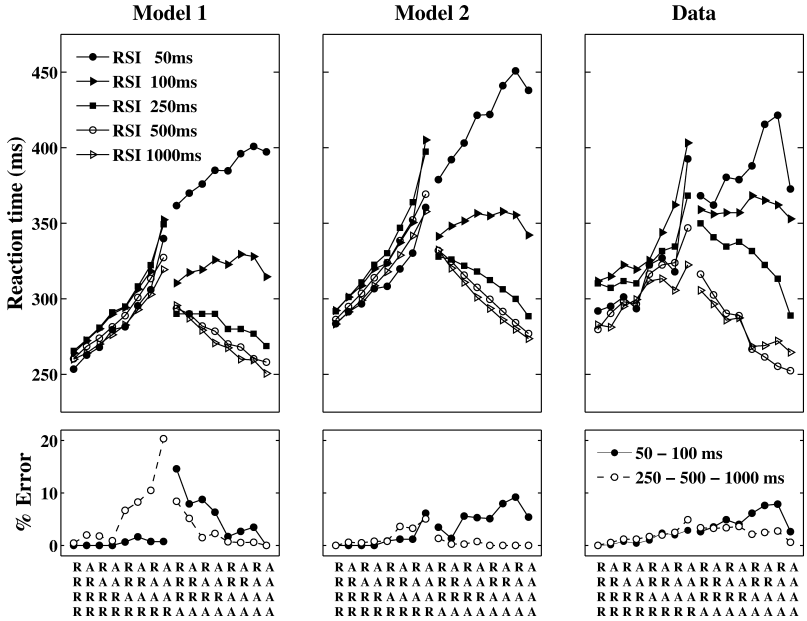

Figure 7: Comparison between model predictions and data under varying RSIs. (Left) Mean RTs (top) and ERs (bottom) for model 1 with noise SD 0.3; conflict implemented by symmetrical inhibitory biases. (Center) RTs (top) and ERs (bottom) for model 2 with noise SD 0.4; conflict acts asymmetrically by decreasing stimulus sensitivity. Averages performed over last trial of sequence histories shown. (Right) Mean RTs (top) and ERs (bottom) from Soetens et al. (1985), reproduced with the authors' permission.

patterns described at the beginning of section 3 that hold across different conditions.

3.3 Comparisons with Additional Data. We end by showing that adjustment of timescales in the model can accommodate effects due to more complex stimuli and to practice.

3.3.1 A More Complex Discrimination Task at Long RSI. Although the transition from AF to SE for both first- and higher-order effects occurs for the same RSI in Soetens et al. (1985) and in the simulation results presented here, this is not necessarily true. In the model, first-order AF is caused by residual activity, but higher-order AF is due to a mechanism similar to that of SE, so the corresponding transition RSI values can differ. Specifically, the timescale of the decision-layer dynamics determines the transition for first-order effects, but the timescales over which conflict and expectation-mediated mechanisms operate determine the transition for higher-order

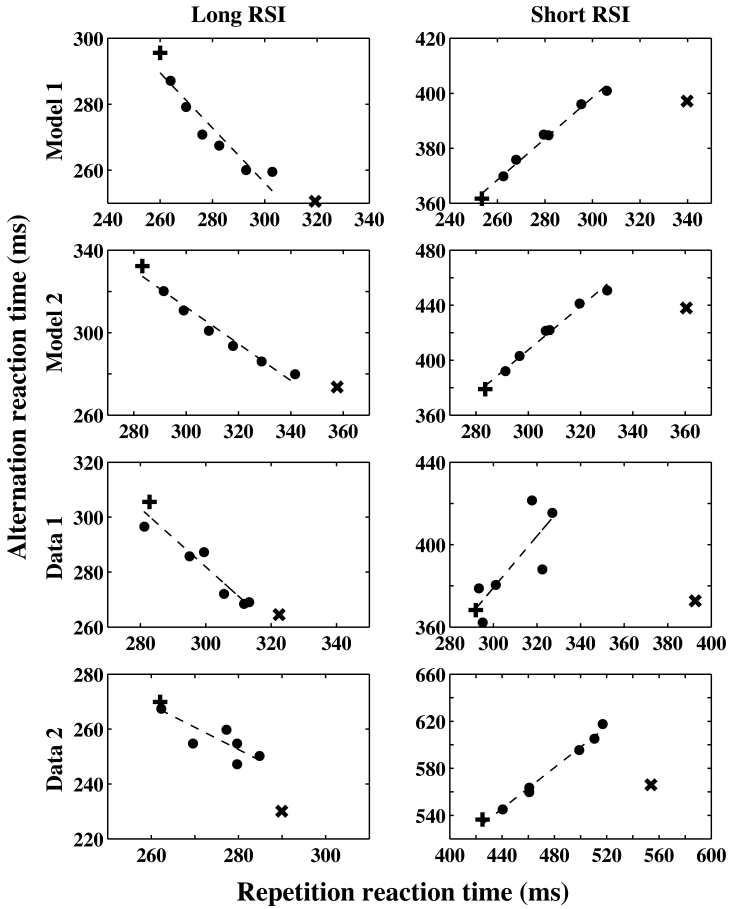

Figure 8: Repetition-alternation scattergraphs. (Top two rows) Scattergraphs for models 1 and 2 with RSI = 1000 ms (left) and 50 ms (right). (Bottom two rows) Scattergraphs for the data of Soetens et al. (1985) (third row), Kirby (1972) (bottom left), and Vervaeck and Boer (1980) (bottom right), presented with authors' or publishers' permissions. Crosses represent the sequence *AAA*, pluses represent *RRR*, and solid circles denote all other sequences. See the opening of section 3 for an explanation. Slopes for long RSIs are negative in both model predictions and data, implying dominance of strategic expectancy (SE); those for short RSIs are positive, implying automatic facilitation (AF).

effects. As noted above, this prediction is confirmed by Cho et al. (2002), which used an 800 ms RSI (see Figure 10). In those data, the first-order effect is dominated by AF, while higher-order SE produces a cost-benefit pattern. This implies that first-order AF persists through the 800 ms RSI, while the transition RSI value from higher-order AF to SE is shorter than 800 ms.

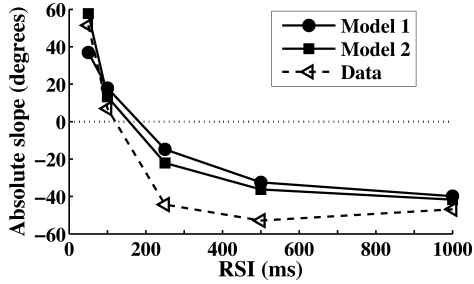

Figure 9: Scattergraph slope dependence on RSI. Slopes (ordinates) decrease from positive, implying dominance of AF, to negative, implying dominance of SE, as RSI increases (abcissa). Filled circles joined by solid line: predictions of model 1 (top row in Figure 8); filled squares joined by solid line: predictions of model 2 (second row in Figure 8); open triangles joined by dashed line: reanalysis of the data of Soetens et al. (1985, Fig. 5) (third row in Figure 8). Transitions from AF to SE occur at about 100 ms for both models and data. An analogous curve representing the bottom panels of Figure 8 cannot be produced due to the lack of data at intermediate RSIs.

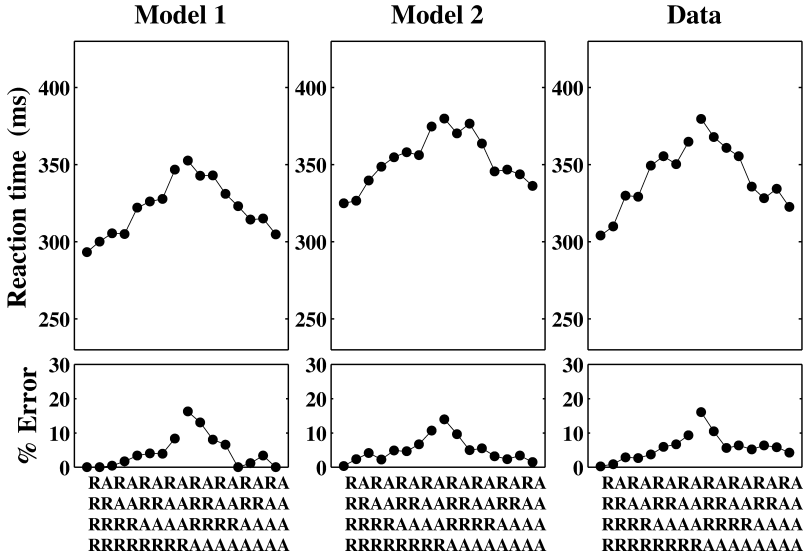

Figure 10: Model fits to the data of Cho et al. (2002). (Left) Mean RTs (top) and ERs (bottom) for model 1 with noise 0.3. (Center) RTs (top) and ERs (bottom) for model 2 with noise SD 0.6. Parameters are as for the previous simulations except for slower post-response decay time constant $\tau_x = 350$ ms and longer nondecision latency $T_{sm} = 200$ ms. Averages performed over last trial of sequence histories shown. (Right) Mean RTs (top) and ERs (bottom) from Cho et al. (2002), reproduced with authors' permission.

The task of distinguishing upper- and lower-case o's in the experiment of Cho et al. (2002) differs from that of Soetens et al. (1985), which is simply to respond to one of two lighted LEDs. The greater task difficulty and longer RTs in Cho et al. (2002) suggest that the decision units would evolve more slowly, but the intrinsic timescale of expectation-mediated bias should not change much, implying longer-lasting residual activity and first-order AF that persists for longer RSIs. We also expect that the visual processing time necessary to decode the case-sensitive stimulus would exceed that for light detection. We confirmed this by changing two parameters. Figure 10 demonstrates that using a slower postresponse decay timescale in equation 2.2 ($\tau_x = 350$ ms in place of 50 ms) and a longer nondecision latency ($T_{sm} = 200$ ms in place of 160 ms), the network with either conflict bias model produces the sequential effect patterns in the data. In increasing τ_x from the 50 ms value chosen in section 2.1.2 (to match Soetens et al., 1985), we are restoring the longer postdecay timescale adopted in Cho et al. (2002).

3.3.2 Practice Changes RT Sequence Patterns. Soetens et al. (1985) also investigated the effects of practice (in experiment 3). In addition to an overall speed-up reflected in reduced RTs that is more marked for short RSIs than for long ones, they find that the slopes and vertical positions of the alternation curves change more than those of repetition curves at the short RSI, while they barely change at long RSI. The overall decrease in reaction time can be intuitively explained by speeding of nondecision sensory-motor processes, the T_{sm} term in our model. Changes in slope and relative position of the alternation curve at short RSI, on the other hand, are often described as the results of a reduction in AF strength (Soetens et al., 1985). With the different mechanisms separated, we can examine these hypotheses. We find that although the first intuition is correct the second is not, in the sense that reduction in conflict-based biasing, the primary mechanism underlying AF, does not produce the observed effects of practice. According to this hypothesis, the slopes of alternation and repetition curves should both be flattened by the same amount. Instead we find that reducing the timescales of all biasing mechanisms can capture the effects.

Specifically, Figure 11 (left, center) shows simulation results when timescales are systematically reduced in stages for the three subsets of data (trial numbers 1–2000, 2001–4000, and 4001–7000). For the second and third subsets, the top-down bias timescales τ and τ_P are reduced to 60% and 40%, respectively, of their original values, mimicking a saturating effect of practice; the postresponse decay timescale of the decision layer, τ_x, is reduced by the square roots of these factors. Consistent with the intuition about the sensory-motor processes, T_{sm} drops from 160 to 140 and 130 ms, respectively. This concerted change of four parameters shows that practice effects are consistent with speed-up of all substages of the process. Faster residual decay could point to more effective resetting of decision units (possibly via basal ganglia; Lo & Wang, 2006), and faster top-down biasing may be due

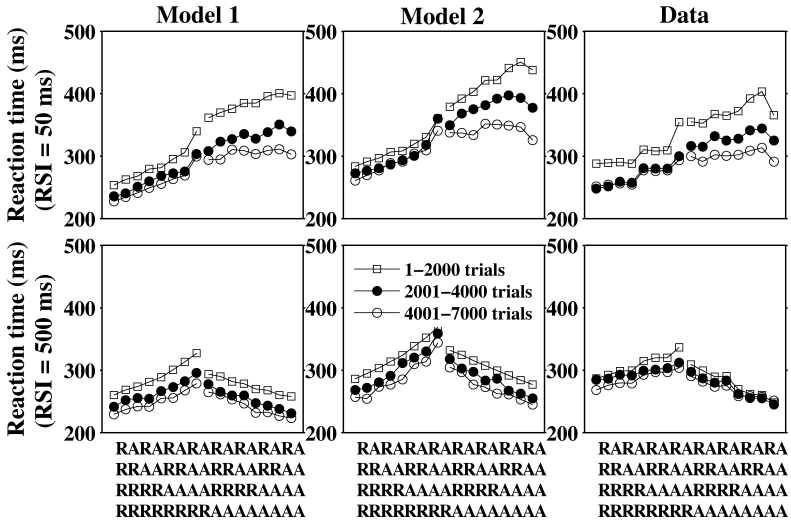

Figure 11: Model fits to practice effects. Each column shows mean RTs for early, middle, and late sets of trials with symbols identified in the key. Top row shows results for 50 ms RSI and bottom row for 500 ms RSI. (Left) Model 1. (Center) Model 2. (Right) Data from Soetens et al. (1985), reproduced with authors' permission. Timescales of the mechanisms of sections 2.1.2–2.1.4 are reduced with practice, as described in text.

to improved effectiveness of memory or conflict inputs (cf. equation 2.8). In addition, since decision-layer activity feeds forward to high-layer control units to produce conflict and expectation, faster decision-layer dynamics also speed up top-down control mechanisms.

4 Discussion

Employing the leaky accumulator model of Usher and McClelland (2001) for decision dynamics, in this article we develop and analyze a unified model of three biasing mechanisms that account for a wide range of phenomena observed in serial RT tasks. In Figure 12 we summarize these mechanisms and their effects on reaction times. On the left, residual activities of the decision units favor repetition over alternation: due to initial condition bias, the current trial takes less time to reach decision threshold if it is a repetition. In the center, asymmetrical biases due to expectation-mediated control lead to a cost-benefit pattern in RTs. At right, both implementations of conflict-induced biases promote a benefit-only pattern in RTs, although the asymmetrical version of model 2 provides better estimates of ERs. Combining these mechanisms, bias due to expectation increases during RSI, while response conflict bias decays, producing the transition from AF to SE.

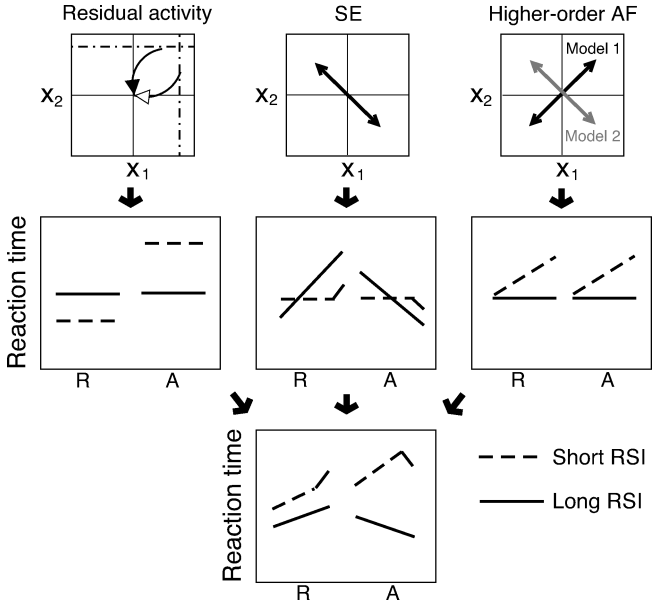

Figure 12: Schematic summary of the three biasing mechanisms. (Top left) Postresponse residual activity of decision units. Black curve with unfilled (filled) arrow shows trajectory during RSI when x_1 (x_2) won previous trial; dash-dotted lines are decision thresholds. (Top center) Asymmetrical bias due to expectation-related priming. (Top right) Biases induced by conflict: black arrow: model 1, symmetrical inhibition; gray arrow: model 2, asymmetrical bias due to decreased stimulus sensitivity. (Middle row) Effects on RT due to individual mechanisms. (Bottom) RT patterns for combined mechanisms: faster dynamics after long alternation sequences causes breakthrough at short RSIs (kinks in dashed lines).

Albeit a model with combined mechanisms may be simpler and seem more appealing, this decomposition permits examination of each individual mechanism's effect, as in Figures 3 to 6, and allows explicit tests of hypotheses and exploration of the influence of different experimental conditions. Specifically, we demonstrate that postresponse decay of neural activity cannot alone account for higher-order AF, but that this can arise from conflict-based inhibition. We then combine the mechanisms to qualitatively reproduce the rich data sets of Soetens et al. (1985), Kirby (1972), and Vervaeck and Boer (1980) in Figures 7 to 9. We confirm our hypothesis that in a more difficult perceptual task, the dynamics of the decision units is slower while that of top-down biases remains largely unchanged (see Figure 10). In particular, by slowing the postresponse decay rate, we explain the dominance of first-order AF and high-order SE at an RSI of

800 ms (Cho et al., 2002). We also find that the overall effects of practice can be accounted for by speed-up of all the mechanisms, without change in the relative strength of conflict-based biases (see Figure 11).

Although the full model includes numerous parameters, few are new to the work presented here, and most of their values, including those of the connectionist model of section 2.1.1, are adopted from the literature (see Table 1). Our numerical experiments revealed that only four parameters require careful tuning to match the data patterns in Figures 7 to 9; specifically, the timescale of the expectancy-mediated control mechanism τ_0 in equation 2.7, the timescale and linear coefficient τ_{p0} and κ of the conflict-mediated control mechanism in equation 2.14, and the ratio of bias strengths due to response conflict and expectation γ_P/γ_B in equations 2.5 and 2.13. The values of these parameters were chosen by hand to lie in reasonable ranges.

Our model does not identify specific brain areas, but it is consistent with functional studies of the anterior cingulate cortex (ACC) and prefrontal cortex (PFC). Specifically, it is known that conflict monitoring is associated with the ACC (e.g., Carter et al., 1998; Botvinick, Nystrom, Fissell, Carter, & Cohen, 1999; Botvinick et al., 2001), and cognitive control is generally thought to involve the PFC (e.g., Botvinick et al., 2001; Johnston & Everling, 2006; Johnston, Levin, Koval, & Everling, 2007). While direct experimental evidence regarding repetition and alternation memories is lacking, we conjecture that they are also based in the PFC, where rule-encoding neurons are known to exist. Indeed, the fMRI study of Huettel, Mack, and McCarthy (2002) found higher PFC activity after pattern violations, with greater amplitudes when longer sequences precede violation. The low time resolution in Huettel et al. (2002) precludes study of detailed dynamics, but the time-resolved EEG study of Sommer et al. (1999) reveals sequential effects in the P300 signal, suggestive of SE for both long (500 ms) and short (40 ms) RSIs, although in the former case, amplitudes are stronger and in the latter case, RTs are unaffected by SE. This suggests that expectation begins to build around 40 ms or earlier. Motivated by this, in section 2.1.3 we adopted a 30 ms delay before onset of expectation-mediated control.

Several potentially important effects were neglected in this study. There is evidence that fast alternations in human subjects could be sensory based rather than mediated by top-down control (Fecteau, Au, Armstrong, & Munoz, 2004). This and other effects could also be (partially) due to an inhibition-of-return phenomenon (Lupianez, Klein, & Bartolomeo, 2006; Klein, 2000; Fecteau & Munoz, 2003). We did not address these or how stimulus-response complexity might modulate biasing mechanisms (Proctor & Vu, 2006; Soetens et al., 1985). Nor did we investigate adjustments to decision thresholds, as in Simen, Cohen, and Holmes (2006), in place of initial conditions and biases. In principle, threshold adjustments can also produce the sequential effect patterns, although the underlying mechanism differs from biasing. (Also see Vickers & Lee, 1998.) We nevertheless hope that our modeling will motivate further behavioral and imaging studies on

humans, as well as electrophysiological primate studies. Sufficiently long trial sequences will be required (e.g., in Dorris, Pare, & Munoz, 2000, only sequences of two prior trials were studied). Conclusive tests of the model will also require new experiments in which RT distributions are collected for a range of RSIs.

In summary, this work offers, for the first time, a unified model that captures and explains a variety of sequential effects observed in serial RT tasks over a wide range of RSIs and experimental conditions. It does so by integrating a mechanistic decision-making model with three essential biasing mechanisms. The different timescales with which these mechanisms operate provide windows into how each contributes to the overall behavior. We believe that this model lays a foundation for addressing sequential effects in more complex tasks and that it offers the opportunity for future experimental assessments.

Acknowledgments

This work was partially supported by PHS grant MH62196 (Cognitive and Neural Mechanisms of Conflict and Control, Silvio M. Conte Center) and AFOSR grant FA9550-07-1-0537. The U.S. government is authorized to reproduce and distribute reprints for governmental purposes, notwithstanding any copyright notation thereon. The views and conclusions contained here are our own and should not be interpreted as necessarily representing the official policies or endorsements, expressed or implied, of the Air Force Research Laboratory or the U.S. government. We thank T. McMillen and E. Soetens for comments and advice and L. Nystrom for sharing experimental data.

References

Audley, R. (1973). Some observations on theories of choice reaction time: Tutorial review. In S. Kornblum (Ed.), *Attention and performance IV*. New York: Academic Press.

Berlyne, D. (1960). *Conflict, arousal, and curiosity*. New York: McGraw-Hill.

Bertelson, P. (1961). Sequential redundancy and speed in a serial two-choice responding task. *Quarterly Journal of Experimental Psychology*, *13*, 90–102.

Bogacz, R., Brown, E., Moehlis, J., Holmes, P., & Cohen, J. D. (2006). The physics of optimal decision making: A formal analysis of models of performance in two alternative forced choice tasks. *Psychological Review*, *113*(4), 700–765.

Botvinick, M., Braver, T., Barch, D., Carter, C., & Cohen, J. D. (2001). Conflict monitoring and cognitive control. *Psychological Review*, *108*, 624–652.

Botvinick, M., Nystrom, L., Fissell, K., Carter, C., & Cohen, J. D. (1999). Conflict monitoring versus selection-for-action in anterior cingulate cortex. *Nature*, *402*, 179–181.

Brown, E., Gao, J., Holmes, P., Bogacz, R., Gilzenrat, M., & Cohen, J. D. (2005). Simple neural networks that optimize decisions. *International Journal of Bifurcation and Chaos*, *15*, 803–826.

Brown, E., & Holmes, P. (2001). Modeling a simple choice task: Stochastic dynamics of mutually inhibitory neural groups. *Stochastics and Dynamics*, *1*(2), 159–191.

Burle, B., Allain, S., Vidal, F., & Hasbroucq, T. (2005). Sequential compatibility effects and cognitive control: Does conflict really matter? *Journal of Experimental Psychology: Human Perception and Performance*, *31*, 831–837.

Burle, B., Roger, C., Allain, S., Vidal, F., & Hasbroucq, T. (2008). Error negativity does not reflect conflict: A reappraisal of conflict monitoring and anterior cingulate cortex activity. *Journal of Cognitive Neuroscience*, *20*, 1637–1655.

Carter, C., Braver, T., Barch, D., Botvinick, M., Noll, D., & Cohen, J. D. (1998). Anterior cingulate cortex, error detection and the on-line monitoring of performance. *Science*, *280*, 747–749.

Cho, R., Nystrom, L., Brown, E., Jones, A., Braver, T., Holmes, P., et al. (2002). Mechanisms underlying dependencies of performance on stimulus history in a two-alternative forced-choice task. *Cognitive, Affective and Behavioral Neuroscience*, *2*, 283–299.

Dorris, M., Pare, M., & Munoz, D. (2000). Immediate neural plasticity shapes motor performance. *Journal of Neuroscience*, *20*, RC52(1–5).

Fecteau, J., Au, C., Armstrong, I., & Munoz, D. (2004). Sensory biases produce the alternation advantage found in sequential saccadic eye movement tasks. *Experimental Brain Research*, *159*, 84–91.

Fecteau, J., & Munoz, D. (2003). Exploring the consequences of the previous trial. *Nature Reviews. Neuroscience*, *4*, 435–443.

Grossberg, S. (1988). Nonlinear neural networks: Principles, mechanisms, and architectures. *Neural Networks*, *1*, 17–61.

Higham, D. (2001). An algorithmic introduction to numerical simulation of stochastic differential equations. *SIAM Rev.*, *43*, 525–546.

Huettel, S., Mack, P., & McCarthy, G. (2002). Perceiving patterns in random series: Dynamic processing of sequence in prefrontal cortex. *Nature Neuroscience*, *5*, 485–490.

Huettel, S., Song, A., & McCarthy, G. (2005). Decisions under uncertainty: Probabilistic context influences activation of prefrontal and parietal cortices. *Journal of Neuroscience*, *25*, 3304–3311.

Jarvik, M. (1951). Probability learning and a negative recency effect in the serial anticipation of alternative symbols. *Journal of Experimental Psychology*, *80*, 243–248.

Jentzsch, I., & Leuthold, H. (2005). Response conflict determines sequential effects in serial response time tasks with short response-stimulus intervals. *Journal of Experimental Psychol.: Human Perception and Performance*, *31*, 731–748.

Jentzsch, I., & Sommer, W. (2001). Sequence-sensitive subcomponents of P300: Topographical analyses and dipole source localization. *Psychophysiology*, *38*, 607–621.

Jentzsch, I., & Sommer, W. (2002). Functional localization and mechanisms of sequential effects in serial reaction time tasks. *Perception and Psychophysics*, *64*, 1169–1188.

Johnston, K., & Everling, S. (2006). Monkey dorsolateral prefrontal cortex sends task-selective signals directly to the superior colliculus. *Journal of Neuroscience*, *26*, 12471–12478.

Johnston, K., Levin, H., Koval, M., & Everling, S. (2007). Top-down control-signal dynamics in anterior cingulate and prefrontal cortex neurons following task switching. *Neuron*, *53*, 453–462.

Jones, A., Cho, R., Nystrom, L., Cohen, J. D., & Braver, T. (2002). A computational model of anterior cingulate function in speeded response tasks: Effects of frequency, sequence, and conflict. *Cognitive, Affective and Behavioral Neuroscience*, *2*, 300–317.

Kirby, N. (1972). Sequential effects in serial reaction time. *Journal of Experimental Psychology*, *96*, 32–36.

Kirby, N. (1976). Sequential effects in two-choice reaction time: Automatic facilitation or subjective expectancy? *Journal of Experimental Psychology: Human Perception and Performance*, *2*, 567–577.

Klein, R. (2000). Inhibition of return. *Trends in Cognitive Sciences*, *4*, 138–147.

Laming, D. (1968). *Information theory of choice reaction times*. London: Academic Press.

Lo, C., & Wang, X.-J. (2006). Cortico-basal ganglia circuit mechanism for a decision threshold in reaction time tasks. *Nature Neuroscience*, *9*, 956–963.

Lupianez, J., Klein, R., & Bartolomeo, P. (2006). Inhibition of return: Twenty years after. *Cognitive Neuropsychology*, *23*, 1003–1014.

Machens, C., Romo, R., & Brody, C. (2005). Flexible control of mutual inhibition: A neural model of two-interval discrimination. *Science*, *307*, 1121–1124.

Melis, A., Soetens, E., & van der Molen, M. (2001). Process-specific slowing with advancing age: Evidence derived from the analysis of sequential effects. *Brain and Cognition*, *49*, 420–435.

Proctor, R. W., & Vu, K.-P. L. (2006). *Stimulus-response compatibility principles: Data, theory, and application*. Boca Raton, FL: CRC Press.

Roitman, J., & Shadlen, M. (2002). Response of neurons in the lateral intraparietal area during a combined visual discrimination reaction time task. *Journal of Neuroscience*, *22*, 9475–9489.

Seung, H. (1996). How the brain keeps the eyes still. *Proceedings of the National Academy of Sciences USA*, *93*, 13339–13344.

Shadlen, M., & Newsome, W. (2001). Neural basis of a perceptual decision in the parietal cortex (area "LIP") of the rhesus monkey. *Journal of Neurophysiology*, *86*, 1916–1936.

Simen, P., Cohen, J. D., & Holmes, P. (2006). Rapid decision threshold modulation by reward rate in a neural network. *Neural Networks*, *19*, 1013–1026.

Soetens, E., Boer, L., & Hueting, J. (1985). Expectancy or automatic facilitation? Separating sequential effects in two-choice reaction time. *Journal of Experimental Psychology: Human Perception and Performance*, *11*, 598–616.

Soetens, E., Deboeck, M., & Hueting, J. (1984). Automatic aftereffects in two-choice reaction time: A mathematical representation of some concepts. *Journal of Experimental Psychology: Human Perception and Performance*, *10*, 581–598.

Soetens, E., & Notebaert, W. (2005). Response monitoring and expectancy in random serial RT tasks. *Acta Psychologica*, *119*, 189–216.

Sommer, W., Leuthold, H., & Soetens, E. (1999). Covert signs of expectancy in serial reaction time tasks revealed by event-related potentials. *Perception and Psychophysics*, *61*, 342–353.

Squires, K., Wickens, C., Squires, N., & Donchin, E. (1976). The effect of stimulus sequence on the waveform of the cortical event-related potential. *Science*, *193*, 1142–1146.

Tversky, A., & Kahneman, D. (1974). Judgement under uncertainty: Heuristics and biases. *Science*, *185*, 1124–1131.

Usher, M., & McClelland, J. (2001). The time course of perceptual choice: The leaky, competing accumulator model. *Psychological Review*, *108*, 550–592.

Vervaeck, K., & Boer, L. (1980). Sequential effects in two-choice reaction time: Subjective expectancy and automatic after-effects at short response-stimulus intervals. *Acta Psychologica*, *44*, 175–190.

Vickers, D., & Lee, M. D. (1998). Dynamic models of simple judgments: I. Properties of a self-regulating accumulator module. *Nonlinear Dynamics, Psychology, and Life Sciences*, *2*, 169–194.

Wang, X.-J. (1999). Synaptic basis of cortical persistent activity: The importance of NMDA receptors to working memory. *Journal of Neuroscience*, *19*, 9587–9603.

Received September 23, 2008; accepted December 17, 2008.